

Polyurethane-based conducting polymer blends

I. Effect of chain extender

K.S. Ho ^{a,*}, K.H. Hsieh ^b, S.K. Huang ^b, T.H. Hsieh ^a

^a Department of Chemical Engineering, National Kaohsiung Institute of Technology, 415 Chien Kung Road, Kaohsiung 807, Taiwan

^b Department of Chemical Engineering, National Taiwan University, Taiwan

Received 28 May 1999; accepted 12 July 1999

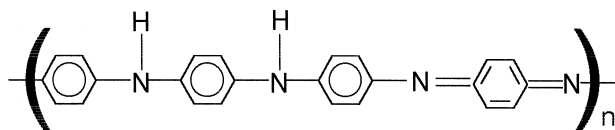
Abstract

Polyurethane (PU) with (*m*-phenylene 4-diaminosulfonic acid: PDSA) as chain extender can deeply influence the properties of its blending with *n*-dodecyl benzene sulfonic acid (DBSA) doped polyaniline (PADB). The sulfonic chain extender (PDSA) provides an additional probability of creating H-bonding with PADB molecules which can be characterized by IR-spectra. In the presence of intermolecular H-bonding, the conductivity and tensile strength of the PADB/PU blends can be changed, especially when the conducting PADB forms a continuous phase in the matrix at high PADB composition. Thermal analysis also reveals variation of glass transition points of the blends at various composition due to the interaction and different degree of miscibility. Scanning electronic microscopy (SEM) pictures of the blends demonstrate a more deformed type of morphology when PDBA is used as a chain extender in the preparation of PU. © 1999 Elsevier Science S.A. All rights reserved.

Keywords: Polyurethane; Chain extender; IR-spectra

1. Introduction

Due to lots of potential application in electronic devices, polyaniline has been widely investigated in the recent years [1,2]. The conducting form of polyaniline can be easily prepared by doping the emeraldine base (EB), which has a half oxidized backbone as illustrated below, with protonic acid resulting in a complex acid salt.



EB

However, most of the conducting doped polyaniline (PADB) is not soluble in regular organic solvents, which make them no difference from other insoluble conducting materials like metallic, or carbon black powders. Polythiophene which is another kind of conducting polymers has

the similar problem was made soluble in organic solvents by covalent-bonded with a long alkyl side chains to each monomer [3]. With the alkylated side chain, the poly(alkyl thiophene) can even be processed like regular thermoplastic polymers [4,5]. Combining the doping and alkylation idea, *n*-dodecyl benzene sulfonic acid (DBSA) which is also a strong protonic acid with a long alkyl chain, was adopted to dope with EB in the solid-form [6] or in solvent [7]. And the resulting DBSA PADB can be soluble in regular organic solvents, such as, CHCl₃, toluene, . . . , etc. The improved solubility makes possible the studies on the conducting polymer blends based on the PADB either by mechanical [8–18] or solution mixing [7]. Kuramoto and Tomita [19] and Cai et al. [20] polymerized the aniline in the presence of DBSA or its salt in chloroform and obtain a homogeneous transparent and green–black suspension solution, which can be a polymer solution for polyblend studies. Owing many H-donor and H-acceptor in the backbones or in the complexed form [21,22], PADB can create various types of H-bonding with other polar polymers such as polyurethane (PU); polycarbonate, . . . , etc. Some of them are capable of building robust H-bonds between different kinds of polymeric molecules. Our studies are focused on preparing a rubbery-like conducting

* Corresponding author

polymer blends based on thermoplastic PU and polyaniline. Expecting the rubbery conducting polyblend can be a material of antenna applied in cellular phone, an anti-static paper roller in a printer, and a fragile, preventive wrapping bag for packing electronic products. The final purpose is to find out the effects of miscibility on mechanical, thermal, and electrical properties of the conducting polyblends.

2. Experimental

2.1. Preparation of PU

PU-prepolymer was prepared with 2:1 mole ratio of purified MDI (4–4' diphenyl methane diisocyanate) to polyol (polytetramethylene oxide:PTMO) at 70°C under nitrogen gas. The obtained PU-prepolymer was mixed with equal moles of chain extender (1.4 Butanediol:1.4 BD or *m*-phenylene 4-diaminosulfonic acid: PDSA) at 70°C until the isocyanate (–NCO groups) disappear in the IR-spectrum, followed by drying in vacuum oven for 3 days. The obtained PUs are designated in Table 1.

2.2. Preparation of DBSA PADB

One liter aniline and ammonia persulfate (APS) separately mixed with 1 M HCl aqueous solution in two plastic bottles were kept in the refrigerator overnight, then the APS solution was added in drop-wise to the aniline HCl solution and kept at 0°–5°C for 24 h with continuous mechanical stirring. The obtained polyaniline was isolated by filtration and dedoped in 0.1 M ammonium water by stirring for 12 h followed by filtration. The wet cake was washed by ethanol and dried in vacuum oven for 3 days and ground into powder by mortar.

PADB was prepared by mixing the dry Pani powders (EB) with DBSA with a weight ratio of 1/2 in chloroform [6]. The mixed solution was filtered and the non-soluble cake was dried and weighted to find out the real concentration of the soluble PADB in chloroform solution.

2.3. Blending

A PU solution in mixed solvents of chloroform and DMF (*N,N* dimethyl formamide) (1:2) was blended with

PADB chloroform solution at various compositions. The obtained polyblend solution was stirred at least 24 h, followed by casting in a petri dish and dried in hood then dried again in a vacuum oven for at least 24 h.

2.4. Characterization

A Bio-Rad FTIR (Fourier-Transform Infrared Spectroscopy:FT-40) was used to characterize PADB and undoped polyaniline (Pani). The scanning ranged from 4000 cm^{-1} to 400 cm^{-1} with 16 times of scanings.

2.5. Testing methods

2.5.1. Tensile strength

The tensile strength was measured by a Tensilon (Mode: TCF-RC, Yashima Works, Japan) followed ASTM D-412 with a crosshead speed of 10 mm/min and at least five specimens were used for the test.

2.5.2. Differential scanning calorimetric (DSC)

DSC thermograms of various samples were obtained from heating the samples from –100°C to 200°C under N_2 purging at 20°C/min by a Du-Pont DSC.

2.5.3. Dynamic mechanical analysis (DMA)

The $\tan \delta$, and E' (of samples were obtained from a Du-Pont DMA at 3°C/min. The sample was 12 × 2 mm and the damping node and frequency are extension and 1 Hz, respectively.

2.5.4. Measurements of conductivity (σ) and normalized σ

Resistance (R) was measured by four-probe method and conductivity was obtained from the formula $\sigma = L/(RA)$ where: L is thickness and A is cross-section area; and σ_n is normalized conductivity which was calculated from $\sigma_n = \sigma/\phi$; where ϕ means weight percent of PADB in PU.

2.5.5. Scanning electronic microscopy (SEM)

Morphological studies were performed by using SEM. Microphotographs were taken of the surface made by fracturing the specimen in liquid nitrogen and then casting it with gold (Au) powder. A HITACHI S-800 SEM was used for morphological observation.

3. Result and discussion

3.1. FTIR-spectra

The undoped polyaniline (EB) which was obtained from neutralization of PADB was characterized by FTIR and shown in Fig. 1.

The strong peak around 3400–3500 cm^{-1} comes from the imino group of Pani and the stretching mode of

Table 1
Designation of PU

PU designation	Polyol employed	Polyol molecular weight	Chain extender employed
PU(PTMO 650B)	PTMO	650	1.4 BD
PU(PTMO 2000B)	PTMO	2000	1.4 BD
PU(PTMO 650P)	PTMO	650	PDSA
Pu(PTMO 2000P)	PTMO	2000	PDSA

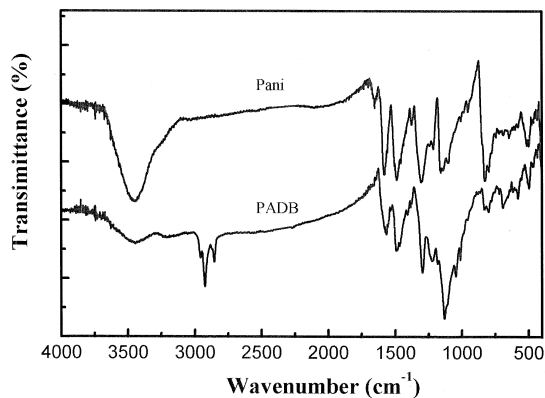


Fig. 1. Infrared spectra of polyaniline before and after doping by dodecylbenzene sulfonic acid.

benzoid and quinoid reveal strong absorptions at 1587 and 1480 cm^{-1} , respectively. The rest absorption peaks are assigned in Table 2.

After being doped by dry DBSA, the IR-spectrum demonstrates a different one, which has the hydrocarbon

Table 2
Assignments of the PADB spectrum

Frequency (cm^{-1})	Assignment
3444	ν (-N-H), free imine
2958	ν (-CH ₃)
2924	ν (-CH ₂ -)
1739-1729 ⁽¹⁶⁾	ν (-C=O), free urethane carbonyl
1713-1706 ⁽¹⁶⁾	ν (-C=O), H-bonded urethane carbonyl
1700	ν (-C=O), free urea carbonyl
<1700	ν (-C=O), H-bonded urea carbonyl
1600	ν (-C=C-), benzene ring
1561	doped ν (-C=N-) of quinoid
1540	δ (N-H) + ν (C-N), amide II
1467	doped ν (-C=C-) of benzoid
1300 ⁽²⁶⁾	ν (-C-N-)
1147	-B-NH-Q-
1135	$\text{H}^+ \text{N} = \text{C}_6\text{H}_4 = \text{N}^+ \text{H}$
1124	-B-NH-B-
1110	ν (-C-O-C-) ether group
1034 ⁽²⁷⁾	ν (-S=O) of -SO ₃ H
1006	ν (-S=O) of -SO ₃ H
801	ν (C-H) para-substituted aromatic out of plain bending

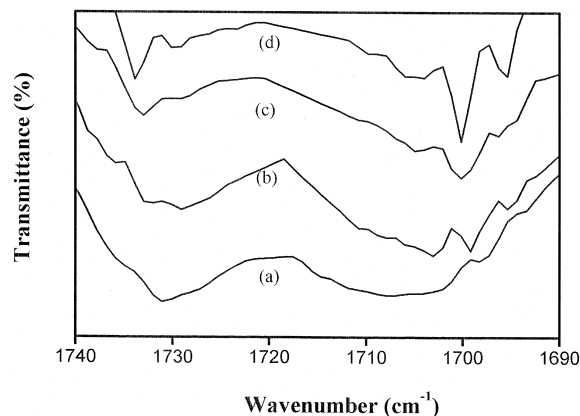


Fig. 2. Infrared spectra of blends with different PANDB/PU(PtMO 650B) ratios: (a) 0/100, (b) 10/90, (c) 30/70, and (d) 50/50.

stretching around 2800–3000 cm^{-1} and the sulfonic stretching absorption at 1185 and 1040 cm^{-1} as illustrated in Fig. 1.

The benzoid and quinoid absorption peaks of DBSA PADB shift to lower wavenumbers after doping due to the created positive charge around the backbones. Other typical absorption are listed in Table 2.

The soluble part of PADB was blended with PU with a co-solvent to check for the affect of chain extender on PADB/PU, FTIR-spectra of PADB/PU blends were performed and illustrated in Figs. 2 and 3. Based on the chemical structure of PU, PADB, and chain extender, the most possible interaction is the H-bonding as displayed in Scheme 1a and c. The carbonyl of the urethane group which owns the typical absorption around 1700 cm^{-1} was used to monitor the H-bonding between same or different types of molecules. The H-bonded carbonyl groups inside PU-molecules can be identified from the splitting speaks of 1734 cm^{-1} and 1705 cm^{-1} (Figs. 2 and 3). The 1734 cm^{-1} absorption represented the free carbonyl and it shifts to 1705 cm^{-1} due to the intermolecular or intramolecular H-bonding of PU-molecules. The incorporated PADB molecules which also has groups being able to induce

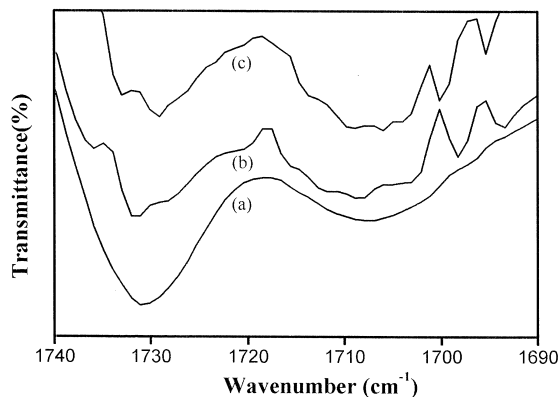
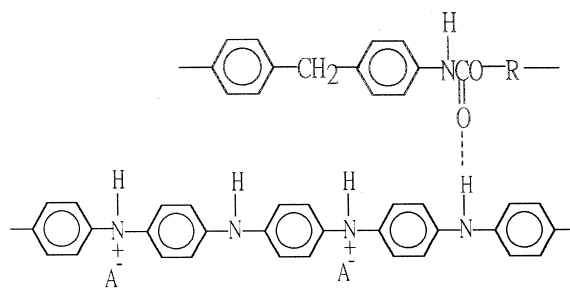


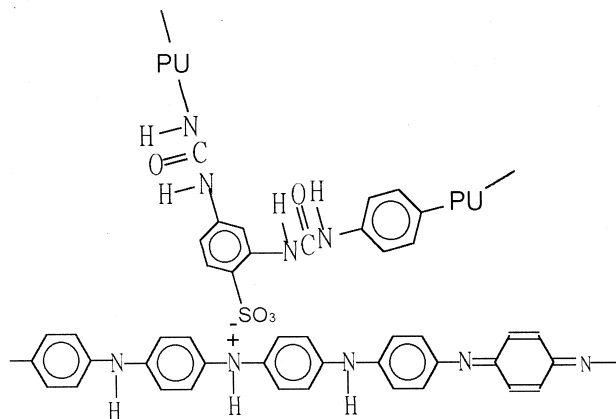
Fig. 3. Infrared spectra of blends with different PANDB/PU(PtMO 650P) ratios: (a) 0/100, (b) 10/90, and (c) 30/70.

(a) intermolecular H-bonding

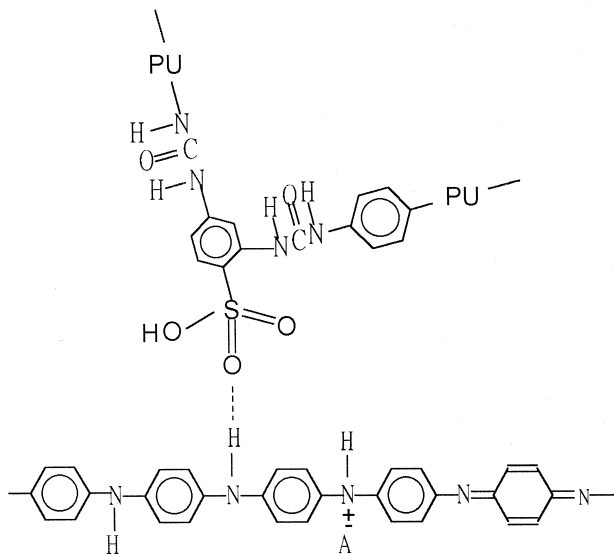


A : DBSA

(b) counter ion interaction



(c) H-bonding



A : DBSA

Scheme 1.

H-bonding can alter the ratio of free or H-bonded carbonyl groups of PU. For PU, which is based on the 1.4 BD chain extender, the H-bonded carbonyl group re-split into more peaks when only 10% of PADB was introduced (Fig. 2b). We can imagine the PADB molecules destroy the H-bond-

ing inside PU molecules and created H-bonding between PU and PADB molecules. Basically, for PU (PTMO 2000B) the only possible type of H-bonding between PU and PADB molecules is the H-acceptor carbonyl group of PU and H-donor imino group of PADB, which is shown in

Table 3
Comparisons of various properties of PADB/PU(P(TMO). Blends with 1.4 BD as a chain extender

Blends	PADB (wt.%)	σ (S/cm)	σ_n (S/cm)	Tensile strength (MPa)	T_g ($^{\circ}$ C)
PU(P(TMO 650B)	0	–	–	15.00	–7
PADB/PU(P(TMO 650B)	10	0.57	5.7	12.90	–6
PADB/PU(P(TMO 650B)	30	8.01	27.0	8.72	–4
PADB/PU(P(TMO 650B)	50	16.0	32.0	7.58	–
PADB/PU(P(TMO 650B)	70	23.5	33.5	7.12	–
PADB	100	74.9	74.9	–	–
PU(P(TMO 2000B)	0	–	–	6.45	–62
PADB/PU(P(TMO 2000B)	10	0.31	3.1	4.48	–59
PADB/PU(P(TMO 2000B)	30	6.15	20.5	3.11	–57
PADB/PU(P(TMO 2000B)	50	12.2	24.4	2.34	–52
PADB/PU(P(TMO 2000B)	70	19.4	27.7	2.77	–
PADB	100	74.9	74.9	–	–

Scheme 1a. The sulfo-group of PADB which is another source of H-acceptor is shielded by the long alkyl chain of doped DBSA and cannot be free to form H-bonding with H-donating group. The H-bonding interaction comes more strongly when more PADB was introduced and the re-splitting of H-bonded carbonyl group at 1705 cm^{-1} of PU was enhanced. Even the number of free carbonyl group at 1734 cm^{-1} was also influenced by the presence of 30% PADB in the blends as shown in Fig. 2c and d. Actually, the free carbonyl groups of PU can be divided into two types. One is called amide (I) [23] which forms the totally free urethane group and does not have any H-bonding with other molecules demonstrating a absorption at 1734 cm^{-1} . The other is the H-bonding between the imine and oxy-groups from two urethanes groups [24,25], which is called amide (II). For PU(P(TMO 2000B), the amide II absorption peak decreases finally when more PADB molecules are introduced as shown in Fig. 2a–d. The strong polar attraction of PADB destroys the bonded between them. When PDSA is used as a chain extender, However, this interaction is somehow enhanced. One possible explanation is due to the lack of carbonyl groups which had been used up during the formation of H-bonds with PADB. And more oxy-groups of urethane are left to create bonding with urethane group.

The splitting of the H-bonded carbonyl at 1705 cm^{-1} when PADB molecules are introduced can be attributed to the various types of imines group of PADB. They include the charged and non-changed imines at least.

For PU(P(TMO 2000P), the interaction is even more complicated due to the presence of urea carbonyl group resulting in different peaks around 1700 cm^{-1} . One of them comes from the H-bonded carbonyl group of the urea. Because there are two kinds of secondary amine groups of urea, they have a large possibility to form H-bond with other groups which also results in more complicated IR-spectra.

The various types of carbonyl absorption around 1700 cm^{-1} for 10% and 30% PADB in PADB/PU(P(TMO 2000P) as illustrated in Fig. 3b and c are due to the presence of urea group shifting these peaks to lower wavenumbers.

When PDSA was used to replace 1.4 BD as a chain extender, each PU-molecule owns one more sulfonic H-acceptor in addition to carbonyl group. It results in the increasing possibility of creating more H-bonds between PU and PADB as displayed in Scheme 1c. That is why the re-splitting of H-bonded carbonyl was more enhanced for PU(P(TMO 2000P) when only 30% PADB was introduced compared with that of PU(P(TMO 2000B) as illustrated in Figs. 2c and 3c. The additional interaction comes from the introduction of sulfuric group at the chain extender can also change the morphology, thermal, mechanical, and even conductivity of PADB/PU blends.

If we specify the spectrum in Fig. 2c, we can find the H-bonded carbonyls of PU(P(TMO 2000B) around 1705 cm^{-1} also disappear when 30% PADB is added. But for PU(P(TMO 2000P) with the same composition (30%), this absorption peak is still significant as illustrated in Fig. 3c. The introduction of PDSA did enhance the H-bonded between different types of molecules (PADB and PU).

3.2. Conductivity and tensile strength

The conductivity and tensile strength of various composition of PADB/PU are separately listed in Tables 3 and 4 and the diagram of σ and tensile strength vs. composition are illustrated in Figs. 4 and 5, respectively. Theoretically, the σ -values will be the same after normalization (σ divided by composition of PADB) if all the PADB molecules in the blends are connected to each other and all contribute to the transport of charge (conductivity) as displayed in Scheme 2c. The assumption is reasonable because the conductivity of pure PU ($10\text{--}10\text{ s/cm}$) is negligible compared to that of pure PADB (74.9 s/cm).

Table 4
Comparisons of various properties of PADB/PU(P(TMO). Blends with PDSA as a chain extender

Blends	PADB (wt.%)	σ (S/cm)	σ_n (S/cm)	Tensile strength (MPa)	T_g ($^{\circ}$ C)
PU(P(TMO 650P)	0	–	–	6.13	–
PADB/PU(P(TMO 650P)	10	0.27	2.7	4.84	–
PADB/PU(P(TMO 50P)	30	5.17	17.2	3.91	–
PADB/PU(P(TMO 650P)	50	11.60	23.2	4.52	–
PADB/PU(P(TMO 650P)	70	16.20	23.0	4.93	–
PADB	100	74.90	74.9	–	–
PU(P(TMO 2000P)	0	–	–	1.89	–63
PADB/PU(P(TMO 2000P)	10	0.71	7.1	2.11	–61
PADB/PU(P(TMO 2000P)	30	6.92	23.1	4.14	–90
PADB/PU(P(TMO 2000P)	50	14.9	29.8	5.13	–57
PADB/PU(P(TMO 2000P)	70	23.70	33.9	5.55	–
PADB	100	74.90	74.9	–	–

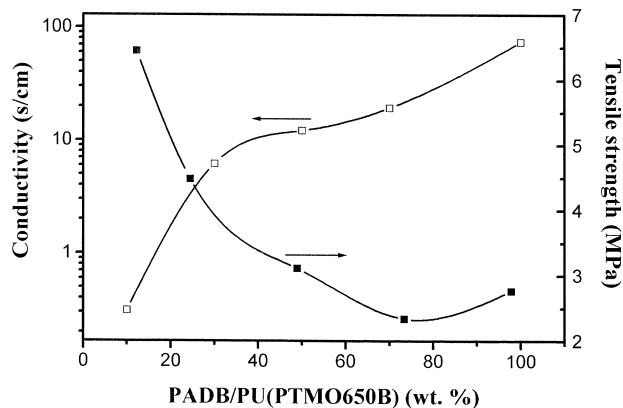
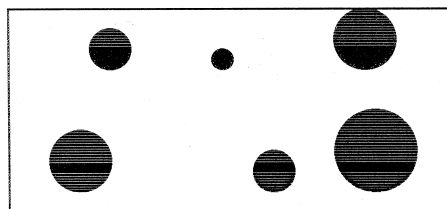


Fig. 4. Conductivity and tensile strength of PANDB/PU(PTMO 650B).

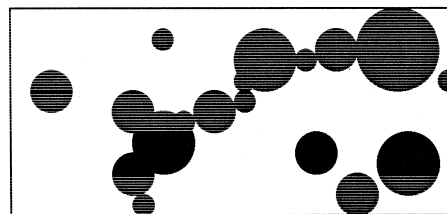
Therefore, we can use the ratio of normalized σ of blends and that of pure PADB to demonstrate the connectivity of PADB molecules in the PADB/PU blends. According to Table 3, when PU is prepared with the 1.4 BD as the chain extender, the connectivity is higher for shorter PTMO diols.

On the contrary, the conductivity increases with the molecular weight of PTMO diols when PDSA is the chain extender in the preparation of PU as listed in Table 4.

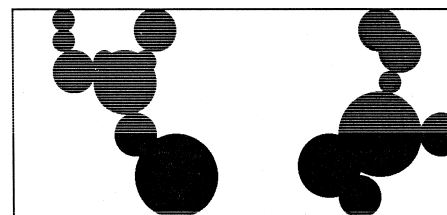
Interestingly, the connectivity (conductivity) does not always contribute to the increase of tensile strength of PADB/PU blends as displayed in Scheme 2a. Fig. 4 illustrates the increase of connectivity (conductivity) results in the decrease of tensile strength of blends when more PADB molecules are introduced. Particularly, when conductivity (connectivity) comes to a sharp increase due to the threshold effect of PADB (percolation) as displayed in Scheme 2a and b, the tensile strength drops more deeply. It indicates that the percolated PADB domain results in an unfavorable effect on strength. And this effect might come from the weaker interaction between PADB and PU(PTMO 2000B). However, for PU(PTMO 2000P), the situation is totally different. According to Fig. 5, the tensile strength increase with conductivity and percentage of PADB. Due to the stronger interaction between PADB



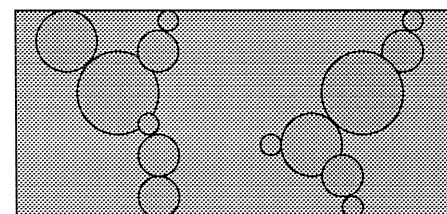
(a) totally disconnected PADB (before percolation)



(b) after percolation



(c) totally connected PADB ($\sigma_n = \sigma_{\text{pure}}$)



(d) partially miscible

The darkness represents the concentration of PADB

Scheme 2.

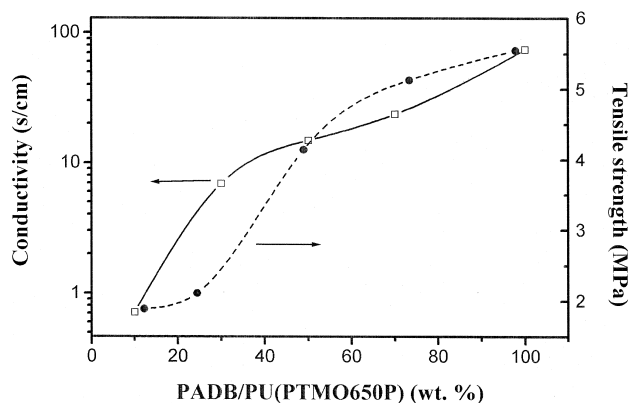


Fig. 5. Conductivity and tensile strength of PANDB/PU(PTMO 650P).

and PU(PTMO 2000P), the tensile strength was enhanced when connectivity of PADB/PU(PTMO 2000P) increases. Both counter ion and H-bonding interaction as shown in Scheme 1b and c contribute to the interaction between the bi-continuous PADB/PU(PTMO 2000P) structure and contribute to the increase of tensile strength.

Note that the sharp increase of tensile strength comes at higher PADB composition compared to the percolation (threshold) of composition as illustrated in Fig. 5. It indicates that the contribution of connected PADB domain can instantly respond to the increase of the conductivity. Slightly higher composition above percolation is not enough to significantly influence the tensile strength. The other possible reason why the normalized conductivity of

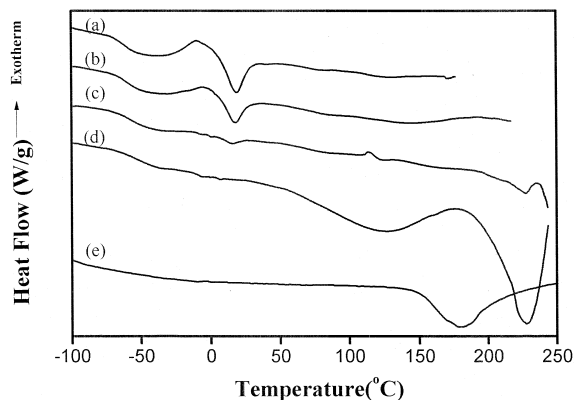


Fig. 6. DSC thermograms of PANDB/PU(PtMO 2000B) blends for various PANDB/PU ratio: (a) 0/100, (b) 10/90, (c) 30/70, (d) 50/50, and (e) 100/0.

PADB/PU(PtMO 2000P) is not be equal to that of pure PADB is because part of the PADB molecules are attracted by the PU molecules and become a miscible phase due to the partially miscible as shown in Scheme 2d. It depends on the degree of miscibility of PADB with PU. In other words, if the individual contribution of PADB-rich and PU-rich domain to conductivity can be measured, the degree of compatibility may be obtained merely from the measurement of the conductivity and morphology.

3.3. Thermal analysis

The thermal analysis by DSC and DMA are performed to characterize the miscibility of PADB/PU blends.

The glassy transition temperatures (T_g) of each types of blend were measured by DSC and illustrated in Figs. 6 and 7, respectively. The glass transition points are separately listed in Tables 3 and 4. The DSC thermogram of pure PADB as illustrated in Fig. 6e demonstrates a strong endothermic peak around 180°C due to the de-doping of DBSA, which detaches from the polyaniline backbones, resulting in the sudden decrease of conductivity of PADB.

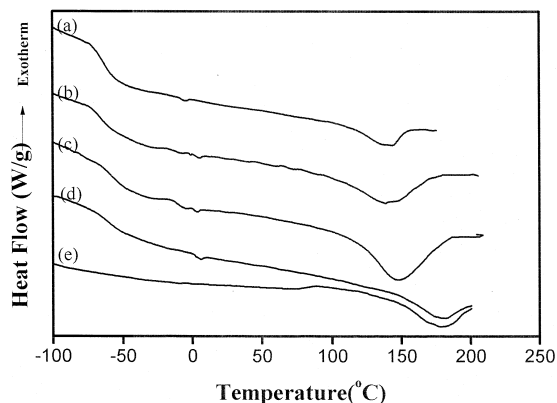


Fig. 7. DSC thermograms of PANDB/PU(PtMO 2000P) blends for various PANDB/PU ratio: (a) 0/100, (b) 10/90, (c) 30/70, (d) 50/50, and (e) 100/0.

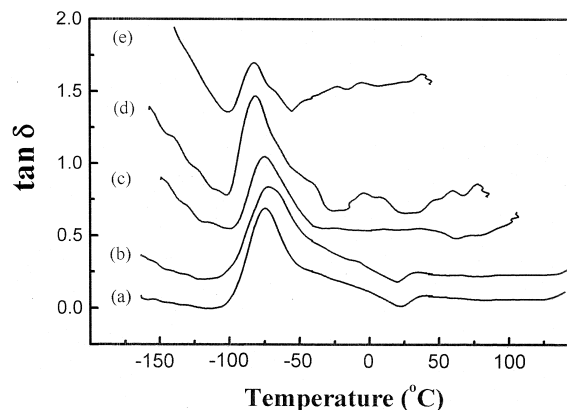


Fig. 8. DMA diagrams of PADB125/PU(PtMO 2000B) (a) 0/100, (b) 10/90, (c) 30/70, (d) 50/50, and (e) 70/30.

The thermogram of pure PU(PtMO 2000B) as illustrated in Fig. 5a reveals a glassy transition temperature around -62°C and a melting peak around 25°C which gradually disappear when more PADB is introduced. It is understood that the long PTM chain can re-crystallize inside PU molecule during quenching when 1.4 BD is used as the chain extender. And the recrystallization is interfered in the presence of PADB (Fig. 6d). This recrystallization is not so significant when PDSA was the chain extender as illustrated in Fig. 7a–d.

The DSC thermogram of PADB/PU(PtMO 2000B) with equal weight (Fig. 6d) demonstrates an endothermic peak of H-bonding around 120°C and a higher de-doping temperature than that of PADB/PU(PtMO 2000P) system. However, this high de-doping temperature does not happen to PADB/PU(PtMO 2000P) system as illustrated in Fig. 7. It seems the high hindrance effect of PDSA as a chain extender cannot protect the DBSA from leaving the backbones at high temperature. And the more flexible backbones of PU with 1.4 BD as a chain extender can accommodate the DBSA molecules and keep it ionic bonded to polyaniline backbone at high temperature. The DSC thermograms of PADB/PU(PtMO 2000P) as illus-

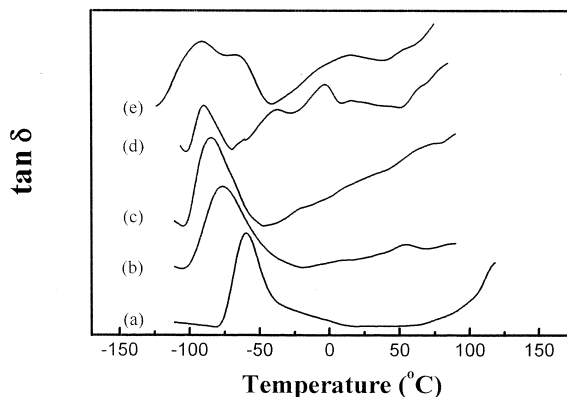
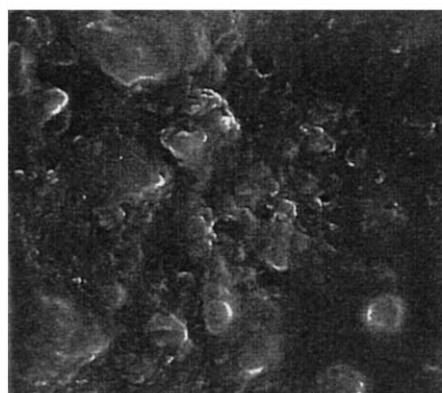


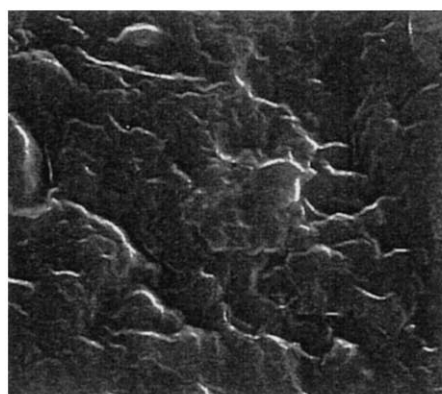
Fig. 9. DMA diagrams of PADB125/PU(PtMO 2000P) (a) 0/100, (b) 10/90, (c) 30/70, (d) 50/50, and (e) 70/30.



(a) Pure PADB



(b) PADB/PU(PTMO 2000B) 50/50



(c) PADB/PU(PTMO 2000P) 50/50

Fig. 10. SEM-pictures of pure PADB, PADB/PU(PTMO 2000B), and PADB/PU(PTMO 2000P).

trated in Fig. 7a–e demonstrate the individual characteristic peaks of pure PU, PADB, and blends. Phase separation might enhance at higher temperature for PADB/PU(PTMO 2000P) system. The glass transition points of the individual blend are listed in Tables 3 and 4, we found that glass transition temperatures (T_g) of the blends increase with the introduction of PADB. However, due to the unavailable T_g of pure PADB, we cannot analyze the miscibility merely from the change of T_g of blends.

DMA was applied to provide more thermal properties of PADB/PU. The $\tan \delta$ vs. temperature for various compositions are illustrated in Figs. 8 and 9. The peak temperature of PU(PTMO 2000B) system as illustrated in Fig. 8 increases more slowly when compared to that of PU(PTMO 2000P) system in Fig. 9. This is another evidence showing the better miscibility between PU(PTMO 2000P) and PADB because this system now owns more types of interaction as shown in Scheme 1b and c.

3.4. Morphological studies (SEM)

Fig. 10a shows the SEM-pictures of pure PADB which has a particle-like structure [8,26]. When PU(PTMO 2000B) is introduced, the particles still exist as shown in Fig. 10b. However, the particles disappear or are deformed when PU(PTMO 2000P) is introduced as shown in Fig. 10c. It is because PU(PTMO 2000P) has a better miscibility with PADB compared to PU(PTMO 2000B).

4. Conclusion

The introduction of PDSA as a chain extender in the preparation of PTMO type PU can influence the properties of PADB/PU blends by the additional H-bonding and counter ionic interaction between sulfonic group of PDSA and PADB. And these interaction can be analyzed by the FTIR-spectra of carbonyl absorption.

The tensile strength of the blends can also increase with the incorporation of PADB which also contribute to the increase of conductivity. Connectivity of PADB rich domain plus the strong interaction between PDSA-chain extended PU and PADB, contribute to the increasing conductivity and tensile strength of PADB/PU(PTMO 2000P). The difference between normalized conductivity of blends and pure PADB can be related to the connectivity and miscibility.

It is possible to monitor the miscibility of conducting polymer blends merely from the conductivity and morphology obtained from microscopy if the individual conductivity of PADB- and PU-rich domain can be justified.

The thermal analysis of blends also demonstrate a better miscibility for PU(PTMO 2000P) with PADB.

SEM-pictures demonstrate the deformation or disappearance of PADB-rich domain in the PADB/PU(PTMO 2000P) system, but not for PADB/PU(PTMO 2000B) system.

References

- [1] A.G. MacDiarmid, A.J. Epstein, Faraday Discuss. Chem. Soc. 88 (1989) 317.
- [2] M. Kaneko, H. Nakamura, J. Chem. Soc., Chem. Commun., 1985, 1441
- [3] R.L. Elsembauer, G.G. Miller, Y.P. Khanna, E. McCarthy, R.H. Banghman, Electrochem. Soc., Ext. Abstr. 85 (1985) 1.
- [4] K.S. Ho, J. Bartus, K. Levon, J. Mao, W.Y. Zheng, J. Laakso, T. Taka, Synth. Met. 55–57 (1993) 384.
- [5] S.A. Chen, J.M. Ni, Macromolecules 25 (1992) 6081.
- [6] K. Levon, K.S. Ho, W.Y. Zheng, J. Laakso, T. Karna, T. Taka, J.E. Osterholm, Polymer 36 (1995) 2733.
- [7] D.C. Liao, K.H. Hsieh, Y.C. Chern, K.S. Ho, Synth. Met. 87 (1997) 61.
- [8] M. Zilbermen, G.I. Titelman, A. Siegmann, Y. Haba, M. Narkis, D. Alperstein, J. Appl. Polym. Sci. 56 (1997) 243.
- [9] Y. Cao, P. Smith, A.J. Heeger, Synth. Met. 48 (1992) 91.
- [10] O.T. Ikkala, J. Laakso, K. Vakiparta, E. Virtamen, H. Ruohonen, H. Jarvinen, T. Taka, P. Passiniemi, J.E. Osterholm, Synth. Met. 69 (1995) 97.
- [11] O.T. Ikkala, T.M. Lindholm, H. Ruohonen, M. Selantaus, K. Vakiparta, Synth. Met. 69 (1995) 135.
- [12] A.J. Heeger, Synth. Met. 55 (1993) 3471.
- [13] Y. Cao, G.M. Treacy, P. Smith, A.J. Heeger, Synth. Met. 57 (1993) 3526.
- [14] Y. Cao, A.J. Heeger, Synth. Met. 52 (1992) 193.
- [15] Y. Cao, P. Smith, A.J. Heeger, Synth. Met. 57 (1993) 3514.
- [16] A. Andreatta, P. Smith, Synth. Met. 55 (1993) 1017.
- [17] P. Passiniemi, K. Vakiparta, Synth. Met. 69 (1995) 237.
- [18] Y. Cao, P. Smith, C. Yang, Synth. Met. 69 (1995) 191.
- [19] N. Kuramoto, A. Tomita, Synth. Met. 88 (1997) 147.
- [20] L.T. Cai, S.B. Yao, S.M. Zhou, Synth. Met. 88 (1997) 209.
- [21] T. Vikki, L.O. Pietilac, H. Osterholm, L. Ahjopalo, A. Takala, A. Toivo, K. Levon, P. Passiniemi, O. Ikkala, Macromolecules 29 (1996) 2945.
- [22] O.T. Ikkala, L.O. Pietilac, P. Passiniemi, T. Vikki, H. Osterholm, L. Ahjopaloc, J.E. Osterholm, Synth. Met. 84 (1997) 55.
- [23] N. Luo, D.N. Way, S.K. Ying, Macromolecules 30 (1997) 4405.
- [24] F.C. Wang, M. Feve, T.M. Lam, J.P. Pascault, J. Polym. Sci., Part B: Polym. Phys. 32 (1994) 1305.
- [25] F.C. Wang, M. Feve, T.M. Lam, J.P. Pascault, J. Polym. Sci., Part B: Polym. Phys. 32 (1994) 1315.
- [26] A.J. Motheo, J.R. Santos Jr., E.C. Venacio, L.H.C. Mattoso, Polymer 39 (1998) 6977.